Journal of Superconductivity and Novel Magnetism
https://doi.org/10.1007/s10948-019-05401-4

ORIGINAL PAPER

Kinetic Inductance in Superconducting Microstructures

K. V. Shein[1] **· V. O. Emelyanova**[1] **· M. A. Logunova**[1] **· A. A. Zarudneva**[1] **· V. V. Zavyalov**[1,2] **· K. Yu. Arutyunov**[1,2]

Received: 8 November 2019 / Accepted: 13 December 2019

Abstract
Simple measuring setup was used to measure high-frequency impedance of superconducting *Ti* and *NbN* microstructures at low temperatures. The shift of resonance frequency below the temperature of superconducting transition compared with the normal state clearly indicates the increase of inductance of the system. The effect is interpreted as the impact of kinetic inductance originating from "inertial" properties of Cooper pairs. Kinetic inductance of superconducting micro and nanostructures should be taken into consideration for various cryoelectronic applications.

Keywords Superconductivity · Microstructures · Kinetic inductance

1 Introduction

Development of modern electronics permanently requires further miniaturization and increase of operational frequency. The first trend leads to severe heat dissipation per unit surface (volume) in conventional CMOS-fabricated micro and nanoscale devices, while the second one claims for mandatory consideration of the frequency-dependent impedance of corresponding elements [1, 2]. To some extent, superconducting electronics [3, 4] can solve the problem of heat dissipation and enables operation of the new generation of nanoelectronic devices such as photon detectors [5] and bolometers [6] taking advantage of rich physics in low-dimensional superconducting systems [7].

Here, we present the experimental study of superconducting *NbN* and *Ti* microstructures at low temperatures. Simple measuring setup was used to measure high-frequency impedance up to 400 MHz enabling determination of the corresponding kinetic inductance.

2 Results and Discussion

Following various sources (for an extensive discussion see, e.g., [8]), one can show that the temperature-dependent kinetic inductance L_k of a superconducting thin film strip with thickness d, length l, and width w ($d << l, d$) can be expressed as:

$$L_k(T) = \left(\frac{l}{w}\right)\frac{R_{sq}}{2\pi\Delta(T)}\tanh\left(\frac{\Delta(T)}{2k_BT}\right) \tag{1}$$

where R_{sq} is the normal state resistance of the film per square area, and $\Delta(T)$ is the temperature-dependent superconducting energy gap. Following Eq. (1), it is easy to conclude that at temperatures well below the critical one $T << T_c$ to obtain the high value of kinetic inductance, one should look either for low-T_c superconductors or for strongly disordered materials with a high value of normal state resistivity. Note that high resistivity in normal state originating from granular structure is a common feature of a vast class of superconductors including high T_cs such as iron-doped materials [9, 10], cuprates [11, 12], and diborides [13]. To study the both limits of low T_c and of highly disordered superconductivity, we have fabricated thin film microstructures of *Ti* and *NbN* (Fig. 1). Critical temperature of superconducting transition of *Ti* films is about $T_c(Ti) = 450$ mK, while for the studied $d = 5$ nm thick *NbN* films, it is about $T_c(NbN) = 6.5$ K (Fig. 2). The normal state resistance per square area for 30-nm thick titanium film can reach $R_{sq}(Ti) \sim 200\ \Omega$ [14, 15] and for 5 nm, *NbN* $R_{sq}(NbN) \sim 1\ \mathrm{K\Omega}$ [1, 5, 16]. Note that in all studied structures,

---

✉ K. Yu. Arutyunov
karutyunov@hse.ru

[1] National Research University Higher School of Economics, Moscow, Russia 101000

[2] P.L. Kapitza Institute for Physical Problems RAS, Moscow, Russia 119334

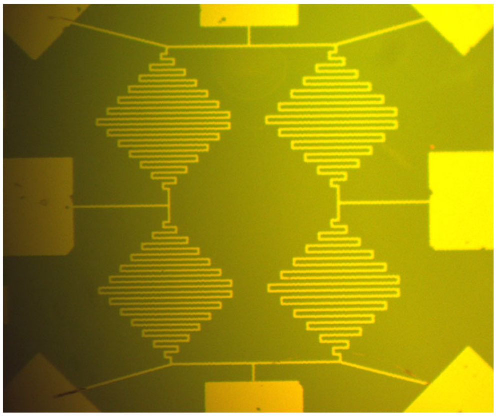

Fig. 1 High-resolution optic microscope image of a typical microstructure: superconducting thin film *Ti* meanders of the same length and thickness, but various line widths. Electron transport properties of each sample can be measured in four-probe configuration

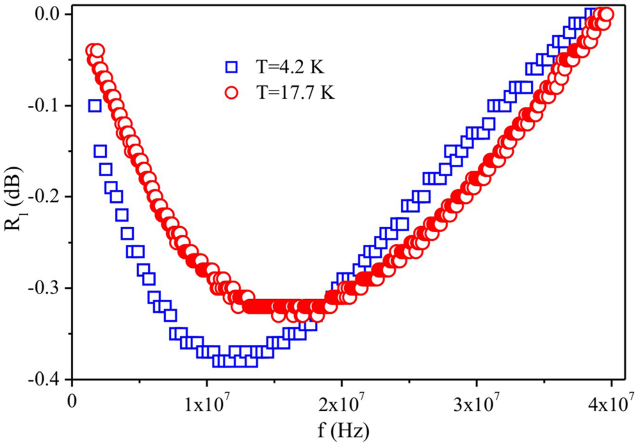

Fig. 3 Return loss R_l vs. frequency *f* for the same *NbN* structure as in Fig. 2 above and below the critical temperature of superconducting transition

the cross section of lines was well above the scales, where at sufficiently low temperatures $T << T_c$, the impact of thermal [7, 17] or quantum phase slip effect is noticeable: both for *Ti* [18, 19] and for *NbN* [16].

Conveniently, one can use network analyzer to determine high-frequency impedance of a circuit. However, in addition to be rather expensive, such commercial devices are not suitable for the measurements of microscopic samples at low temperatures without proper attenuation of the probing signal. Here, we have used simple and cheap setup similar to the one used for measuring amplitude-frequency characteristics of various RF filters [20]. Both the current in the circuit and the voltage across the inductor could be registered simultaneously (Fig. 1). The output of RF generator was loaded through 50 Ω cryogenic-graded coaxial cable by the *LC* circuit, where *L* is the unknown inductance of the microstructure and $C = 50$ pF is the known value of parallel connected "ballast" capacitor (Fig. 3, inset). The separate measurements of the capacitor proved that its capacitance does not change much from room temperature down to 2 K at frequencies up to 400 MHz.

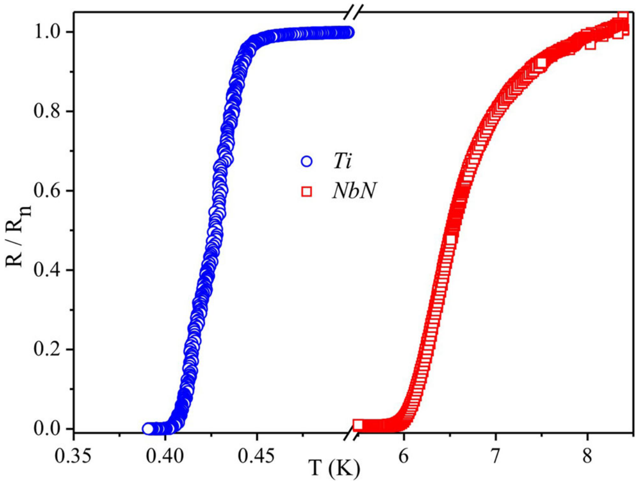

Fig. 2 Typical resistance normalized by normal state value R/R_n vs. temperature *T* dependencies for *Ti* (○) and *NbN* (□) microstructures

In our experiments, we measured the return loss R_l as the function of the probing signal frequency. It can be evaluated as

$$R_l[dB] = -20\log_{10}\left|\frac{Z_{\text{load}}-Z_{\text{source}}}{Z_{\text{load}}+Z_{\text{source}}}\right| \quad (2)$$

where Z_{load} and Z_{source} are the impedances of the load and source, correspondingly. The dependencies $R_l(f)$ clearly demonstrate minimum, corresponding to the resonant frequency f_{rez} of the system (Fig. 3). The shift of f_{rez} to lower values with cooling the system to superconducting state indicates the increase of the impedance of the system. Given that the ballast capacitance is constant $C = 50$ pF, the value of the total inductance can be trivially deduced: $L = L_k + L_m = (1/4\pi^2 C)(1/f_{rez})^2$. L_m is the magnetic inductance which is determined solely by the geometry of the system and, hence, is identical in normal and superconducting states.

For thin film *NbN* meander with length $l = 500$ µm, thickness $d = 5$ nm, and line width $w = 100$ nm "packed" into 10 um (micrometer) by 10 um (micrometer). area from $R_l(f)$ dependency (Fig. 3), one can evaluate the total inductance at $T = 4.2$ K as $L = L_k + L_m \approx 5.07$ µH. The corresponding kinetic inductance per unit area in superconducting state is $L_k \approx 0.76$ nH/□. Our results on *NbN* structures are in reasonable quantitative agreement with the earlier results [1, 2, 8, 21]. Slightly higher values of specific kinetic inductance compared with [8, 21] can be accounted to further increased disorder in our *NbN* films resulting in higher resistivity ($R_{sq} \approx 1$ kΩ against 875 Ω) and lower critical temperature ($T_c = 6.5$ K against 10 K).

Qualitatively similar results were obtained on the *Ti* samples. However, complicity with measurements at ultra-low temperatures in $^3He^4He$ dilution refrigerator resulted in rather messy amplitude-frequency dependencies. The exact origin of this parasitic effect is not yet clear. For example, it might be related to frequency-dependent overheating of titanium microstructures at ultra-low temperatures. Further experimental activity is required for unambiguous interpretation of the *Ti* data.

3 Conclusions

Simple measuring setup was used to measure high-frequency return losses of *NbN* and *Ti* microstructures at cryogenic temperatures. The clearly observed shift of the resonance to lower frequencies below the critical temperature of superconducting transition is interpreted as the impact of kinetic inductance providing the noticeable impact only in superconducting state. The value of kinetic inductance per unit area for the *NbN* samples is in a reasonable agreement with the literature data. Unambiguous interpretation of *Ti* data needs further experimental activity.

Acknowledgements The authors would like to acknowledge the SCONTEL team and personally, A. A. Korneev for the fabrication of NbN samples, and A. Yu. Kuntsevich and V. I. Chichkov for training the students (V. O. Emelyanova, M. A. Logunova, and A. A. Zarudneva).

Funding Information The article was prepared within the framework of the Academic Fund Program at the National Research University Higher School of Economics (HSE) in 2019–2020 (grant no. 19-01-050) and by the Russian Academic Excellence Project "5-100."

References

1. Kerman, A.J., Dauler, E.A., Keicher, W.E., Yang, J.K.W., Berggren, K.K., Gol'tsman, G., Voronov, B.: Appl. Phys. Lett. **88**, 111116 (2006)
2. Kerman, A.J., Dauler, E.A., Yang, J.K.W., Rosfjord, K.M., Anant, V., Berggren, K.K., Gol'tsman, G.N., Voronov, B.M.: Appl. Phys. Lett. **90**, 101110 (2007)
3. H.J.M. ter Brake, F.-Im. Buchholz, G. Burnell, T. Claeson, D. Crété, P. Febvre, G.J. Gerritsma, H. Hilgenkamp, R. Humphreys, Z. Ivanov, W. Jutzi, M.I. Khabipov, J. Mannhart, H.-G. Meyer, J. Niemeyer, A. Ravex, H. Rogalla, M. Russo, J. Satchell, M. Siegel, H. Töpfer, F.H. Uhlmann, J.-C. Villégier, E. Wikborg, D. Winkler and A.B. Zorin: Physica C **439**, 1 (2006).
4. Tolpygo, S.K., Bolkhovsky, V., Rastogi, R., Zarr, S., Day, A.L., Golden, E., Weir, T.J., Wynn, A., Johnson, L.M.: IEEE Trans. Appl. Supercond. **29**, 1102513 (2019)
5. Korneeva, Y., Vodolazov, D.Y., Semenov, A.V., Florya, I., Simonov, N., Baeva, E., Korneev, A., Goltsman, G., Klapwijk, T.M.: Phys Rev Appl. **9**, 064037 (2018)
6. Kuzmin, L.S., Blagodatkin, A.V., Mukhin, A., Pimanov, D.A., Zbrozhek, V.O., Gordeeva, A.V., Pankratov, A.L., Chiginev, A.V.: Supercond. Sci. Technol. **32**, 035009 (2019)
7. Arutyunov, K. Yu., Golubev, D.S., Zaikin, A.D.: Phys. Rep. **464**, 1 (2008)
8. Annunziata A J : Ph.D. dissertation, Yale University (2010).
9. Ricci, A., Poccia, N., Campi, G., Joseph, B., Arrighetti, G., Barba, L., Takano, Y.: Phys. Rev. B. **84**(**6**), 060511 (2011)
10. Ricci, A., Poccia, N., Joseph, B., Innocenti, D., Campi, G., Zozulya, A., Takeya, H.: Phys. Rev. B. **91**(2), 020503 (2015)
11. Campi, G., Bianconi, A., Poccia, N., Bianconi, G., Barba, L., Arrighetti, G., Burghammer, M.: Nature. **525**(7569), 359 (2015)
12. Fratini, M., Poccia, N., Ricci, A., Campi, G., Burghammer, M., Aeppli, G., Bianconi, A.: Nature. **466**(7308), 841 (2010)
13. Agrestini, S., Metallo, C., Filippi, M., Simonelli, L., Campi, G., Sanipoli, C., Latini, A.: Phys. Rev. B. **70**(13), 134514 (2004)
14. Arutyunov, K. Yu., Lehtinen, J.S.: Nanoscale Res. Lett. **11**, 364 (2016)
15. Elo, T., Lähteenmäki, P., Golubev, D., Savin, A., Arutyunov, K., Hakonen, P.J.: J. Low Temp. Phys. **189**, 204 (2017)
16. Arutyunov, K. Yu., Ramos-Álvarez, A., Semenov, A.V., Korneeva, Y.P., An, P.P., Korneev, A.A., Murphy, A., Bezryadin, A., Gol'tsman, G.N.: Nanotechnology. **27**, 47LT021 (2016)
17. Arutyunov, K. Yu., Ryynanen, T.V., Pekola, J.P., Pavolotski, A.B.: Phys. Rev. B. **63**, 092506 (2001)
18. Lehtinen, J.S., Arutyunov, K. Yu.: Supercond. Sci. Technol. **25**, 124007 (2012)
19. Arutyunov, K. Yu., Lehtinen, J.S., Rantala, T.: J. Supercond. Nov. Magn. **29**, 569 (2016)
20. Zavyalov, V.V., Chernyaev, S.A., Shein, K.V., Shukaleva, A.G., Arutyunov, K. Yu.: J. Phys. Conf. Ser. **969**, 012086 (2017)
21. Annunziata, A.J., Santavicca, D.F., Frunzio, L., Catelani, G., Rooks, M.J., Frydman, A., Prober, D.E.: Nanotechnology. **21**, 445202 (2010)